Available online at www.sciencedirect.com
SCIENCE DIRECT®
Bulletin of Mathematical Biology 67 (2005) 663–682
Bulletin of Mathematical Biology
www.elsevier.com/locate/ybulm

Coupled map lattice approximations for spatially explicit individual-based models of ecology

Å. Brännström*, D.J.T. Sumpter

Mathematics Department, Umeå University, SE-901 87 Umeå, Sweden

Received 7 November 2003; accepted 29 September 2004

Abstract

Spatially explicit individual-based models are widely used in ecology but they are often difficult to treat analytically. Despite their intractability they often exhibit clear temporal and spatial patterning. We demonstrate how a spatially explicit individual-based model of scramble competition with local dispersal can be approximated by a stochastic coupled map lattice. The approximation disentangles the deterministic and stochastic element of local interaction and dispersal. We are thus able to understand the individual-based model through a simplified set of equations. In particular, we demonstrate that demographic noise leads to increased stability in the dynamics of locally dispersing single-species populations. The coupled map lattice approximation has general application to a range of spatially explicit individual-based models. It provides a new alternative to current approximation techniques, such as the method of moments and reaction–diffusion approximation, that captures both stochastic effects and large-scale patterning arising in individual-based models.

1. Introduction

Spatially explicit individual-based models are commonly used to understand and study the behaviour of ecological systems (DeAngelis and Gross, 1992; Czaran, 1998; Diekmann et al., 2000). Applications of these models have been both phenomenological, where general properties of ecological systems are elucidated through the study of a model

* Corresponding author.
E-mail address: ake.brannstrom@math.umu.se (Å. Brännström).

0092-8240/$30
doi:10.1016/j.bulm.2004.09.006

(Ermentrout and Edelstein-Keshet, 1992; Nowak and May, 1992; Boerlijst et al., 1993; Bolker and Grenfell, 1995; Pacala and Tilman, 1996; Iwasa et al., 1998; Keeling et al., 2000), and quantitative, where specific predictions about a system can be made and direct comparisons drawn to an experimental or field-based system (Keeling et al., 2001; Kerr et al., 2002). The strength of individual-based modelling is that direct observations of how individuals act and interact can be specified and included in a model, thus forcing precise thinking and developing intuition about how the studied system functions.

It is often difficult to treat spatially explicit individual-based models analytically. An intriguing question therefore is whether it is possible to approximate their qualitative behaviour in a small number of analytically tractable equations. To address this problem, Rand and Wilson (1995) used delay embedding techniques to show that the dynamics of a spatial resource-predator–prey model could be captured in a set of four differential equations. In a similar spirit, Pascual and Levin (1999) describe a spatial predator–prey model and show that when sampling of the population is made at the appropriate spatial scale the dynamics are well approximated by two differential equations. Such observations are encouraging since they indicate that, on some spatial scale at least, the population dynamics of spatial individual-based models can be approximately equivalent to those of a small number of differential equations.

Broadly speaking, there are two well established approximation techniques for the reduction of spatially explicit individual-based models: the *reaction–diffusion approximation* and the *method of moments*. The reaction–diffusion approximation deals with models where individuals follow a random walk and are so abundant that their distribution can be regarded as continuous in space (Murray, 1989, Chapter 9). Diffusion approximations break down when the stochastic behaviour of a few individuals becomes important. For example, if reproduction takes place at discrete times while dispersal is a continuous diffusion process then population spread can in reality be determined by small numbers of individuals jumping ahead of a travelling wave rather than by an assumed population wave front (Mollison, 1991; van Baalen, 2000).

The method of moments (Bolker and Pacala, 1997) accounts for the local spatial correlations which can arise from discrete events. The dynamics of the spatial distribution are approximated by studying how the mean, variance and (possibly) higher moments of this distribution evolve in time. A first-order moment approximation assumes that the population is well-mixed and stochastic fluctuations can be ignored, resulting in a non-spatial system of ordinary differential equations. A second-order approximation includes evolution equations for the variance as well as the mean, and is often sufficient to capture much of the spatial correlation in the system, both quantitatively and qualitatively. The technique of *pair approximation* (Sato and Iwasa, 2000; van Baalen, 2000) is essentially the method of moments applied to probabilistic cellular automata. Second-order pair approximation involves estimating differential equations for the rate of change of pairs of neighbouring cells in a cellular automata, thus capturing how local correlations between neighbouring cells evolve.

Second-order moment methods typically fail to capture any large-scale emergent patterns, such as spiral waves or checkerboard patterns, that are often seen to arise out of spatially explicit individual-based models [see Johnson and Boerlijst (2002) for examples of such large-scale patterns]. By their nature, such patterns give rise to large higher-order

moments, corresponding to skew or bimodality in the spatial distribution. Accounting for third-order moments becomes highly cumbersome and produces approximations that are difficult to understand and not guaranteed to give any useful information about the spatial distribution (Bolker et al., 2000). While some of these large-scale patterns might be captured by a reaction–diffusion approximation, the problems associated with stochastic actions of small numbers of individuals remains. There thus exists a large class of spatial individual-based models for which we currently have no means of approximating and establishing analytical understanding.

Here we develop a third alternative approximation technique aimed at establishing at least some analytical understanding of spatially explicit individual-based models with large-scale emergent patterns. We call this approach a *coupled map lattice approximation*. To illustrate its application we use an example of a model that exhibits checkerboard patterns and chaotic oscillations. We begin by describing the individual-based model, then its coupled map approximation and ultimately compare the model and the approximation with an aim to understanding how local dispersal stabilises the population dynamics.

2. Model and approximation

2.1. The spatially explicit individual-based model

The model we study here is a local-dispersal extension of one proposed by Sumpter and Broomhead (2001) for the parasitism of honey bee brood cells by *Varroa* mites. Although our model is no longer appropriate for *Varroa* mite reproduction—since mites disperse globally rather than locally between reproductive phases—it would be realistic for modelling the reproduction of other species exhibiting scramble competition over discrete resource sites, such as the bean bruchid *Callosobruchus phaseoli* (Toquenaga and Fujii, 1991). Our model is also of interest from a theoretical perspective since, for a wide range of parameter values, it exhibits checkerboard pattern oscillations as well as chaotic cycles. Indeed, the model gives a simple illustrative example of how simple reproductive competition can give rise to complex community level dynamics (Johnson and Boerlijst, 2002).

In the model, individuals 'live' on an $n \times n$ lattice of resource sites, which will henceforth be referred to as a 'world'. The world has cyclic boundary conditions, so that individuals leaving the 'top' or 'right-side' of the world reappear on the 'bottom' or 'left-side' respectively and vice versa. Mathematically this means that we identify two sites (i, j) and (i', j') if both $i - i'$ and $j - j'$ are multiples of n. We let C_{ij}^t denote the number of individuals at site (i, j) at time t. Individuals reproduce and disperse in two discrete phases (see Fig. 1).

The reproduction phase involves local competition for a resource site. To each site we apply an interaction function $\phi : \mathbb{Z} \mapsto \mathbb{Z}$. The interaction function acts on the site content C_{ij}^t to give a new site population, $\phi(C_{ij}^t)$. In the current model we define

$$\phi(k) = \begin{cases} b & \text{if } k = 1 \\ 0 & \text{otherwise} \end{cases} \tag{1}$$

giving a classic scramble competition model (Nicholson, 1954): one individual at a site produces b offspring, but if there is more than one individual at a site then all individuals

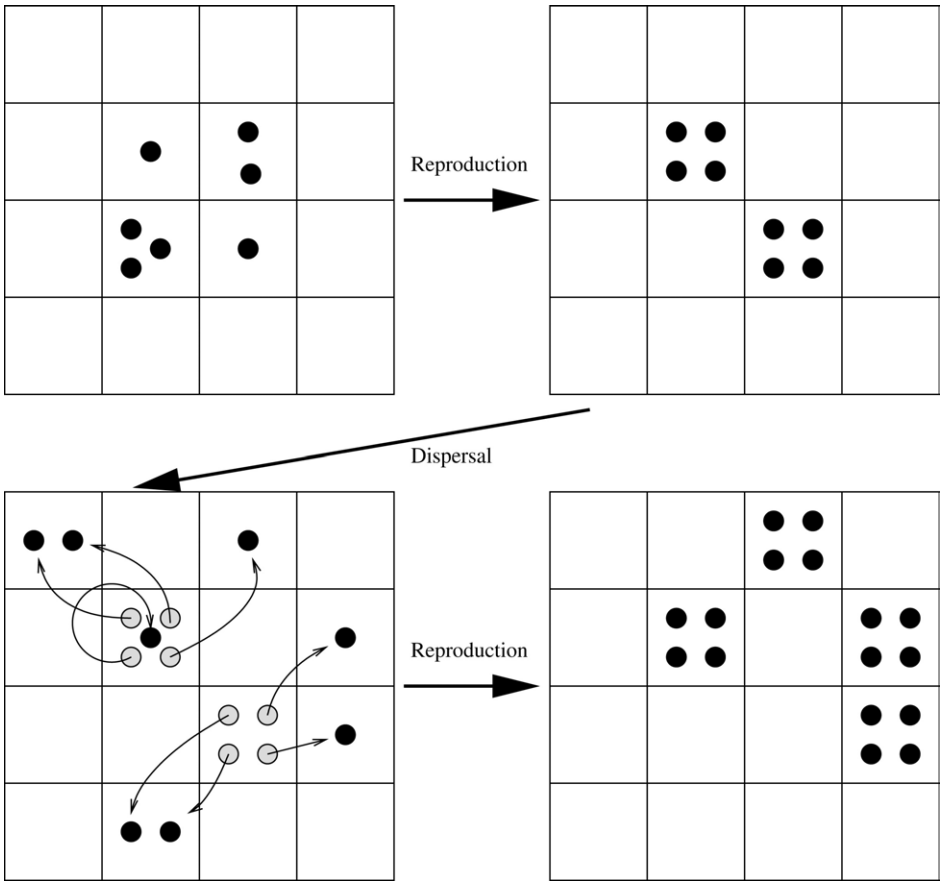

Fig. 1. The spatially explicit individual-based model. Each box represents a site, and individuals are represented by black circles. Shown are the reproductive phase where sites with exactly one individual produce $b = 4$ offspring followed by dispersal where individuals disperse in a range $s = 1$ and then once more reproduction. If two or more individuals share the same site they fail to reproduce due to interference.

fail to reproduce due to interference. Although we consider only Eq. (1) here, the interaction can easily be extended to incorporate other forms of competition, interactions between more than one species and stochasticity in the number of offspring produced (Johansson and Sumpter, 2003).

After reproduction, each of the $\phi(C_{ij}^t)$ individuals disperse. In this dispersal phase individuals choose a site uniformly at random from a local neighbourhood of $(2s+1) \times (2s+1)$ sites, where s is the maximum distance an individual can disperse. Throughout this paper we will assume that $(2s+1) \leq n$ so that there can be no multiple covering of the same site by dispersal. We now make this concept precise. Recall that we identify two sites (i, j) and (i', j') if both $i - i'$ and $j - j'$ are multiples of n. Define the neighbourhood $\mathrm{N}(i, j, s)$ as the set of sites for which there exists a representation $(i', j') \in \mathbb{Z}^2$ such that $|i - i'| \leq s$ and $|j - j'| \leq s$. The local population M_{ij}^t is defined as the number of

individuals in the local neighbourhood to site (i, j) after reproduction, i.e.,

$$M_{ij}^t = \sum_{(i',j')\in \mathrm{N}(i,j,s)} \phi(C_{i'j'}^t).$$

The dispersal gives rise to a new site count $\{C_{ij}^{t+1}\}$ with

$$\mathrm{P}(C_{ij}^{t+1} = k \mid M_{ij}^t = m) = \binom{m}{k} \frac{1}{(2s+1)^{2k}} \left(1 - \frac{1}{(2s+1)^2}\right)^{m-k}. \tag{2}$$

In addition to the local population, we define the total population M^t

$$M^t = \sum_{1\le i,j\le n} \phi(C_{ij}^t).$$

In most cases it is more convenient to work with densities instead of absolute population numbers. Thus we define $X^t = M^t/n^2$.

2.2. The normal approximation

When the dispersal area equals the size of the world, i.e., when $n = 2s + 1$, the individuals disperse uniformly over all sites. This specific well-mixed case can be described by a mean-field approximation, which we now derive. Using that $M_{ij}^t = M^t$ we get

$$\begin{aligned}\mathrm{E}[M^{t+1} \mid M^t = m] &= \sum_{1\le i,j\le n} \sum_{k=0}^{m} \phi(k)\mathrm{P}(C_{ij}^t = k \mid M^t = m) \\ &= \sum_{1\le i,j\le n} \sum_{k=0}^{m} \phi(k) \binom{m}{k} \left(\frac{1}{n^2}\right)^k \left(1 - \frac{1}{n^2}\right)^{m-k}.\end{aligned}$$

Letting $n \to \infty$ while keeping the density $x = m/n^2$ constant gives

$$\Phi(x) := \mathrm{E}[X^{t+1} \mid X^t = x] = \exp(-x) \sum_{k=0}^{\infty} \phi(k) \frac{x^k}{k!}.$$

Furthermore, Johansson and Sumpter (2003) have shown that when $X^t = x$, $n = 2s + 1$ and $n \to \infty$ the random variable

$$\frac{1}{n}\left[\sum_{1\le i,j\le n} \phi(C_{ij}^t) - n^2 \Phi(x)\right]$$

converges in distribution to a normal distribution with mean 0 and variance

$$v(x) = \mathrm{Var}[\phi(U_x)] - x\,\Phi'(x)^2$$

where U_x is a Poisson distributed random variable with expectation x. This means that when n is large the population density X^{t+1} is well approximated by the *stochastic normal approximation*

$$x^{t+1} = \Phi(x^t) + \frac{\sqrt{v(x^t)}}{n}\epsilon^t \tag{3}$$

where $\epsilon^t \sim \mathrm{N}(0, 1)$.

When applied to the specific interaction function in Eq. (1) we have that

$$\Phi(x) = bx\exp(-x) \tag{4}$$

and

$$v(x) = b^2x\exp(-x)(1-\mathrm{e}^{-x}) + b^2x^2\exp(-2x)(1-x). \tag{5}$$

Eq. (4) is the well-known Ricker map (Ricker, 1954; May, 1976), and rigorous basic dynamical facts for the Ricker map can be found in Thunberg (2001). The Ricker map has the fixed points $x_1^* = 0$ and $x_2^* = \ln b$. As the parameter b increases, the map goes through a series of period doubling bifurcations with the first occurring when $b = e^2$ [for this value $\Phi'(x_2^*) = -1$]. Eventually, at approximately $b = 15$, an accumulation point is reached and chaos ensues. Regions with periodic dynamics occur for higher values of b, but in our experience the addition of a stochastic term often causes complicated dynamics even for these values.

Although Eq. (3) is obtained as $n \to \infty$, it does in practice provide a good approximation when the scramble interaction function Eq. (1) is used, even for small n. We expect this to hold for many other interaction functions as well.

2.3. The coupled map lattice approximation

When the dispersal area does not cover the entire world, the spatial structure becomes important and Eq. (3) fails to provide a good approximation of the population dynamics. However, if we consider a subsection of the world comparable in size to the dispersal range, it is reasonable to assume that locally the individuals are approximately well-mixed after accounting for the fact that individuals will enter and leave through the boundary. This is the intuitive idea that we build upon. Assume that the world can be divided up into patches of equal size $s \times s$, where s is as before the maximal dispersal range of an individual. The reason for this choice of patch size is that it is the largest size that preserves the maximum propagation speed of individuals in the system. In these patches we assume the individuals to be well-mixed so that the stochastic normal approximation applies. The patches are then coupled with diffusion, corresponding to the dispersal of individuals that takes place in the spatially explicit individual-based model. As can be seen from Fig. 2, after dispersing from a given patch, there are nine possible patches where the individual may subsequently be found. This is the basis for the coupled map approximation, which we now put in mathematical terms.

Assuming that s divides n we index the $l = n^2/s^2$ patches in the lattice. Let $X^t = (X_1^t, \ldots, X_l^t)$, where X_i^t is interpreted as the density of individuals at patch i. The coupled map lattice (CML) approximation is then written as

$$X^{t+1} = D(R(X^t, \epsilon^t), \gamma^t) \tag{6}$$

where ϵ^t and γ^t are vectors of independent random variables with standard normal distribution of length l and $9l$ respectively. The functions R and D correspond to reproduction and diffusion respectively. We now define these functions.

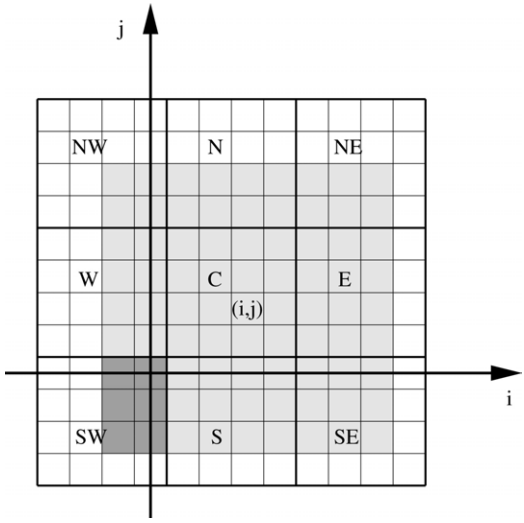

Fig. 2. The grey area shows the sites reachable by dispersal from site (i, j) when $s = 4$. Since dispersal is uniform the fraction of dark grey to light grey sites in the figure is the probability that an individual at site (i, j) disperse to patch SW. For $s = 4$ the probability that an individual placed at random in patch C disperse to patch SW is, with an accuracy of two decimals, $d_{SWC} = 0.08$. The corresponding values for dispersal from patch C to C and W respectively are $d_{WC} = 0.12$ and $d_{CC} = 0.20$. In the general case, the probabilities or diffusion coefficients are given by Eqs. (9)–(11).

2.3.1. Reproduction

To describe the reproductive phase we assume that Eq. (3) provides a good approximation to the actual reproductive outcome at each patch. This would be the case if the individuals at each patch are uniformly distributed. We then define the function $R : \mathbb{R}^l \times \mathbb{R}^l \mapsto \mathbb{R}^l$ component-wise as:

$$R_i(x, \epsilon) = \left(\Phi(x_i) + \frac{\sqrt{v(x_i)}}{s} \epsilon_i \right)^+ \tag{7}$$

where $(x_i)^+$ is the maximum of x_i and 0, while $\Phi(x_i)$ and $v(x_i)$ are defined in Eqs. (4) and (5) respectively.

2.3.2. Diffusion

To complete the formulation we need to define the function representing the diffusion due to dispersal. Assume that each patch i contains m_i individuals, and that after dispersal the number of individuals at patch i is the random variable M_i. If we let $\kappa(i)$ denote the nine patches in the Moore-neighbourhood of i, depicted in Fig. 2 with the central patch C representing patch i, we can write

$$M_i = \sum_{j \in \kappa(i)} D_{ij}$$

where D_{ij} is the number of individuals dispersing to patch i from patch j. We assign to each individual k in patch j a Bernoulli variable I_k which is 1 if the individual disperses

from patch j to patch i and 0 otherwise. Then, assuming a total of m_j individuals in patch j,

$$D_{ij} = \sum_{k=1}^{m_j} I_k.$$

Define d_{ij} as the probability that an individual placed at random in patch j disperse to patch i. If the individuals at patch j are uniformly distributed, then D_{ij} is distributed binomially as $\mathrm{Bin}(m_j d_{ij}, m_j d_{ij}(1-d_{ij}))$. This can be approximated with a normal distribution, i.e.,

$$D_{ij} \approx m_j d_{ij} + \sqrt{m_j d_{ij}(1-d_{ij})}\gamma_{ij}$$

where $\gamma_{ij} \sim \mathrm{N}(0,1)$. To ensure that we will not have negative populations we take the maximum of 0 and D_{ij}. Then

$$M_i \approx \sum_{j\in\kappa(i)} \left[d_{ij} m_j + \sqrt{m_j d_{ij}(1-d_{ij})}\gamma_{ij} \right]^+.$$

The CML approximation in Eq. (6) is expressed in terms of population densities rather than total population numbers. We thus divide with s^2 and write $X_i = M_i/s^2$, $x_i = m_i/s^2$ to give a component-wise definition of $D : \mathbb{R}^l \times \mathbb{R}^{9l} \mapsto \mathbb{R}^l$:

$$D_i(x,\gamma) = \sum_{j\in\kappa(i)} \left[d_{ij} x_j + \sqrt{\frac{x_j}{s^2} d_{ij}(1-d_{ij})}\gamma^{ij} \right]^+. \tag{8}$$

Note that diffusion, as defined here, is not conservative. We also implemented the coupled map lattice approximation with conservative diffusion, but apart from longer simulation times, there were no noticeable difference between the two. Possibly, the introduction and removal of individuals through non-conservative diffusion is of minor importance when compared to births and deaths that occur at each patch.

To implement the diffusion step we need explicit values for the diffusion coefficients. Recall that d_{ij} is the probability that an individual placed at random in patch i disperse to patch j. This is actually a simplification as individuals are really distributed in 'packets' of b individuals each. We first determine the value of the diffusion coefficient d_{SWC} for uniform dispersal and diffusion from a patch C to the southwest neighbouring patch SW (see Fig. 2). Assume that there are m uniformly distributed individuals in patch C about to disperse, and recall that each individual disperses to any of $(2s+1)^2$ sites in a square around the individual with uniform probability. Assign, as before, a Bernoulli variable I_k to each individual k in the central patch, which is 1 if the individual disperses to any of the sites in the southwest patch SW and 0 otherwise, i.e., I_k is 1 with probability d_{SWC}. If we index the sites in C by (i,j), $1 \le i, j \le s$ then from the assumptions just made, it follows that

$$\begin{aligned} d_{SWC} &= \sum_{1\le i,j\le s} \frac{1}{s^2} \times \mathrm{P}(k \text{ disperse to patch SW} \mid \mathrm{k \text{ at } } (i,j)) \\ &= \sum_{1\le i,j\le s} \frac{1}{s^2} \times \frac{\#\text{ reachable sites in patch SW}}{(2s+1)^2}. \end{aligned}$$

Thus, in our example in Fig. 2 we need to find the overlap (marked in dark grey) between the neighbourhood of size $(2s+1)^2$ around (i, j) and the southwest patch SW. The southwest patch SW covers sites (i', j') where $-s+1 \leq i', j' \leq 0$. Using these facts, we get

$$d_{SWC} = \sum_{1 \leq i,j \leq s} \frac{1}{s^2} \frac{(s+1-i)(s+1-j)}{(2s+1)^2}$$
$$= \frac{1}{s^2(2s+1)} \sum_{i=1}^{s} (s+1-i) \left(\sum_{j=1}^{s} (s+1-j) \right).$$

By reindexing, the sum in large brackets is just $\sum_{j=1}^{s} j = \frac{1}{2}s(s+1)$. Hence,

$$d_{SWC} = \frac{(s+1)^2}{4(2s+1)^2}. \tag{9}$$

A similar argument shows that the coefficient for diffusion from C to C is

$$d_{CC} = \frac{s^2}{(2s+1)^2} \tag{10}$$

and finally from C to W,

$$d_{WC} = \frac{s(s+1)}{2(2s+1)^2}. \tag{11}$$

As $s \to \infty$, these tend to $1/16$, $1/4$ and $1/8$ respectively.

The preceding derivation of diffusion is based on dispersal in a square neighbourhood. In practice, the coupled map lattice approximation will work for most local dispersal functions and for other topologies, provided the patch size is small enough that individuals can be assumed locally well-mixed. For example, if we used geometric dispersal, where individuals perform an uncorrelated random walk, we would have to consider diffusion to all other patches. However, the probability of dispersal decreases exponentially with distance and we could possibly consider dispersal only to patches where the diffusion coefficient exceeds some threshold value. Thus, while other forms of dispersal may make an actual implementation more complex, the coupled map lattice approximation could still be applied.

2.3.3. The deterministic coupled map lattice approximation

We define the deterministic version of the coupled map lattice approximation as

$$X^{t+1} = \overline{D}(\overline{R}(X^t)) \tag{12}$$

where $\overline{D}(x) = D(x, 0)$ and $\overline{R}(x) = R(x, 0)$, where 0 is the zero vector of suitable dimension. This is a standard (forward) diffusive coupled map lattice model.

2.4. Implementation

The spatially explicit individual-based model was implemented using the software package Swarm, while the coupled map approximation was implemented in Matlab. The diffusion coefficients were calculated using Eqs. (9)–(11).

2.5. Computational complexity

Although theoretically both the complexity of the individual based model and the coupled map lattice approximation is $O(n^2)$, as each individual or patch requires a constant number of operations, the approximation was in practice much faster overall. For example, although the coupled map lattice approximation was implemented in Matlab, 80% of the computation time required to produce Fig. 5 was spent calculating data for the individual based model.

3. Results

Fig. 3 shows how the distribution of individuals evolves over time for three time steps of the individual-based model, for various parameter values. When the dispersal is very local ($s = 3$) and the number of offspring is relatively low [Fig. 3(a)], we see high spatial variation in the population density within generations. However, between generations the spatially averaged population density is almost stable [Fig. 4(a)]. When dispersal takes place over a wider range, the spatial population density is relatively homogeneous within each generation [Fig. 3(b)], but period 2 oscillations occur in the average population density over consecutive generations [Fig. 4(b)]. When the number of offspring per individual is large, then checkerboard patterns appear, where highly populated areas on one time step become sparsely populated on the next [Fig. 3(c)]. In this case, the average population density can exhibit chaotic oscillations (not shown, but see below).

Fig. 4 compares the time series from three different individual-based simulations with those generated by the CML approximation [Eq. (6)] and the deterministic CML [Eq. (12)]. For these parameter values, the CML approximation appears to recreate the population dynamics of the individual-based model. The deterministic CML, however, always converges to the mean approximation Eq. (4), as all of the coupled maps become entrained. Indeed, since diffusion reduces the differences between neighbouring sites, one can show that the synchronised state is a stable attractor of Eq. (12). The stochastic terms in Eq. (6) are thus essential in replicating the dynamics of the individual-based model.

The stochastic coupled map lattice accurately approximates the long-term population dynamics of the individual based model for a wide range of parameter values. Fig. 5 shows 'bifurcation plots', where the long-term distribution of populations values for both the spatially explicit individual-based model and its coupled map lattice approximation are plotted against the number of offspring b, for various values of s. For these values of s and b, Fig. 5 also shows the difference between the mean of the time-series from the individual-based model and coupled map lattice approximation and the difference in variance. Especially for $s = 2$ and $s = 3$, there is a small difference in mean, which seems to depend linearly on b. This is likely an artefact due to the use of the normal approximation, Eq. (3), for very few sites (four and nine, respectively). The variance is also similar, but there is a clear deviation around $b = 10$ when periodic dynamics occur. However, with the exception of $s = 3$, the approximation is reasonably accurate for values of b in the region where the mean approximation, $\Phi(x)$, has its first series of period doubling bifurcations, i.e., for approximately $b < 15$. The anomaly at $s = 3$ is caused by it being close to a 'bifurcation point', where the global population goes from being

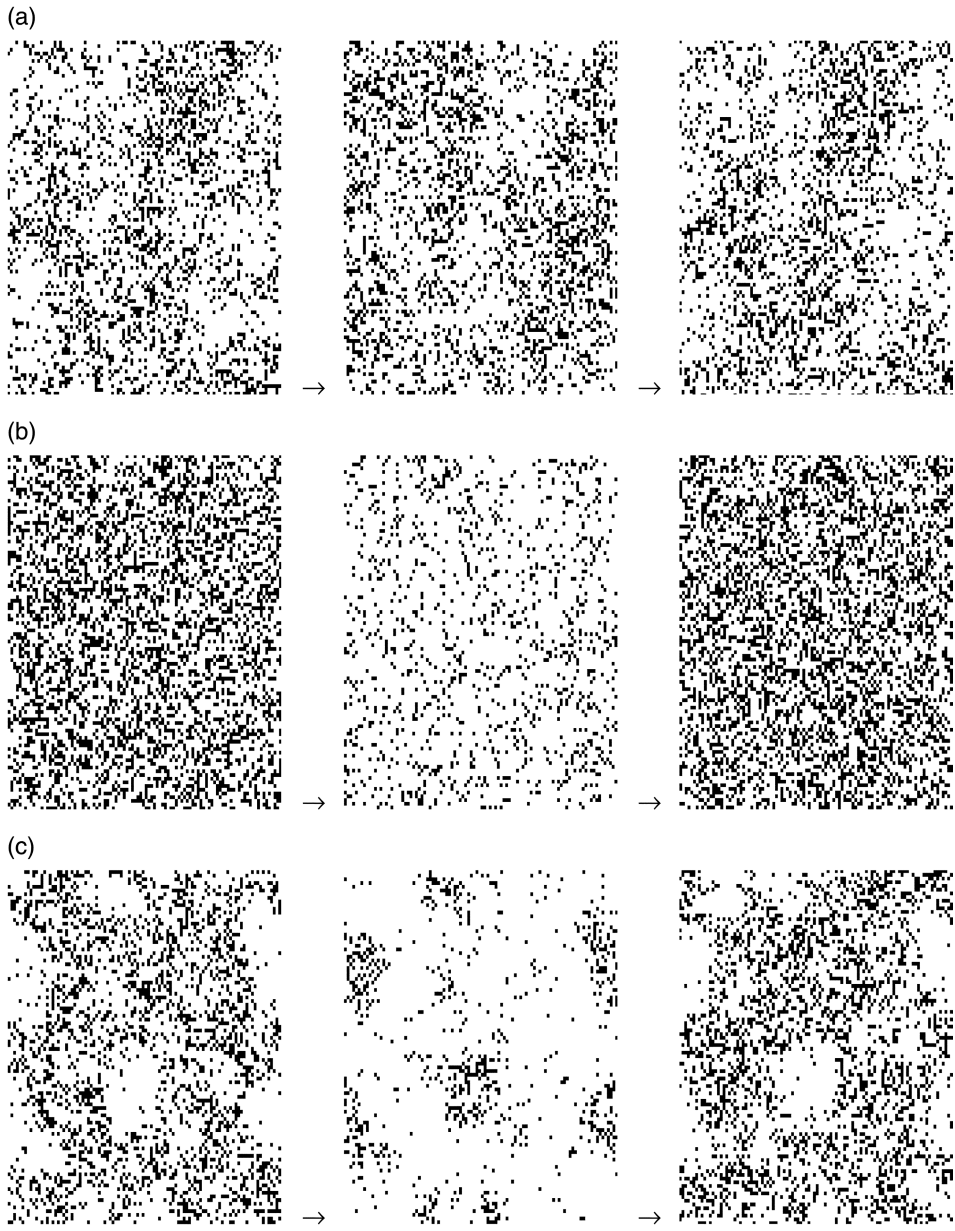

Fig. 3. Three consecutive snapshots of the individual-based simulations with parameters (a) $b = 10$ and $s = 3$, (b) $b = 10$ and $s = 5$ and (c) $b = 20$ and $s = 5$.

stable to exhibiting period 2 oscillations. Indeed, if we fix $b = 10$ and change s, as in Fig. 6, we see that $s = 3$ is close to the point at which periodic oscillations appear.

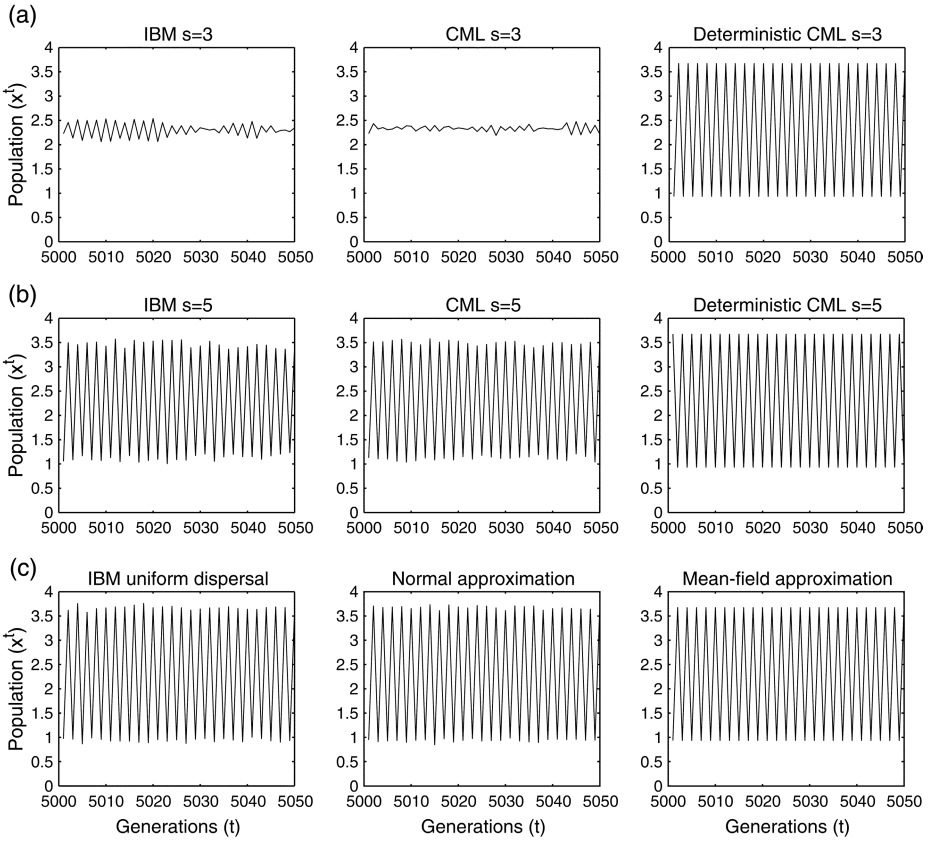

Fig. 4. Time-series sampled after 5000 generations from the individual-based model (IBM, left column), the coupled map lattice approximation (CML, middle column) and the deterministic coupled map lattice approximation (Deterministic CML, right column) with parameters $n = 100$ and (a) $b = 10$ and $s = 3$, (b) $b = 10$ and $s = 5$ and (c) $b = 10$ and $s = n/2 - 1$, i.e., uniform dispersal.

For $b > e^2 (\approx 7.39)$, if dispersal is global, i.e., $s = n/2 - 1$, then the population density exhibits oscillations between generations. Fig. 6 shows a shift from stable to periodic population dynamics as the dispersal range increases, both in the individual-based simulation and in the coupled map lattice approximation. For local dispersal the population density can be stable across generations, while as s increases the population tends to behave in a similar manner to the case where dispersal is global [e.g., compare Fig. 4(b) and (c)]. Local dispersal can thus be said to stabilise population dynamics.

Approximately when $b > 15$ and the dispersal is global the population often has chaotic dynamics. Fig. 3(c) shows a typical sequence of spatial distributions for local dispersal: checkerboard patterns appear, where local areas alternate between containing very high and very low population densities. With b in this region, the CML fails to provide quantitative predictions of the behaviour of the individual-based model (Fig. 7). However, both the CML and the individual-based model exhibit either stable or periodic dynamics, whereas

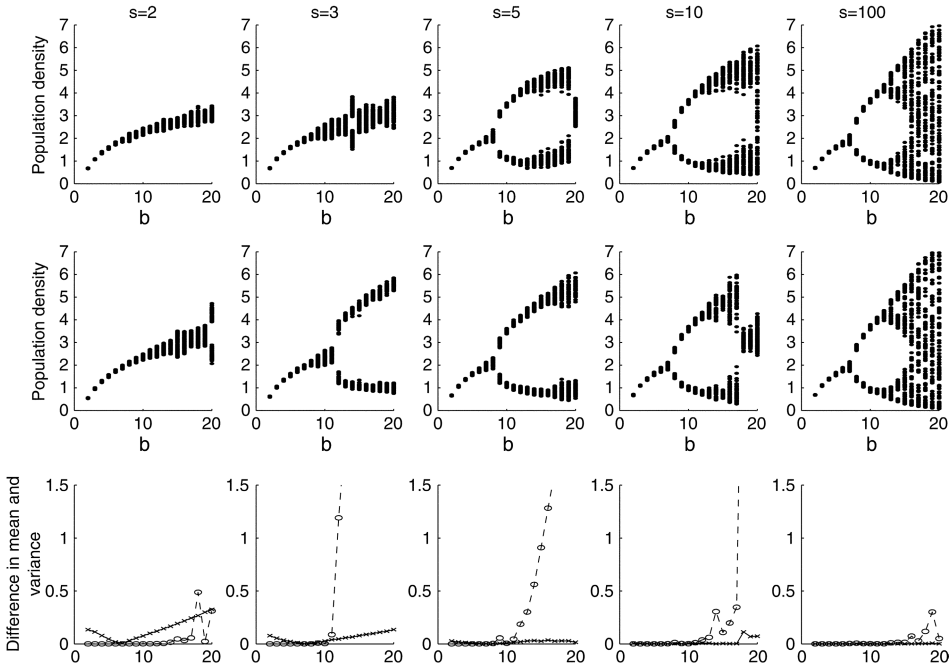

Fig. 5. 'Bifurcation plots' comparing the individual-based model (top row) and its coupled map lattice approximation (middle row) for five different values of the dispersal range s. For each s, the parameter n is set to the integer multiple of s closest to 100, i.e., $n = 100, 99, 100, 100, 100$ for the five plots respectively. To produce the bifurcation plots we simulated 5000 generations for each b and plotted the population density of the last 100 generations. The bottom row of plots were produced by taking the absolute value of the difference between the mean of the last 1000 iterations of the time-series from the individual based model and the mean of the last 1000 iterations of the time-series from the coupled map lattice approximation (crosses) as well as the corresponding absolute value of the difference in variance (circles and dashed line).

the normal-approximation and global dispersal models predict chaotic dynamics. Again, local dispersal plays a stabilising role in the population dynamics, this time causing chaotic oscillations to become stable or periodic.

4. Analysis

The general pattern revealed by the simulations of both the coupled map lattice and the individual-based model is that shorter dispersal ranges correspond to greater spatial variation but less temporal variation in the population dynamics. There is furthermore a rapid shift from stable to periodic population dynamics as the dispersal range increases. To understand the effect of local dispersal on population dynamics we consider a simple system of l globally coupled patches where reproduction is followed by diffusion and added stochasticity. Let $X^t = (X_1^t, \ldots, X_l^t)$. Given $\epsilon^t = (\epsilon_1^t, \ldots, \epsilon_l^t)$, a vector of independent and N(0, 1)-distributed random variables, the system can be written as

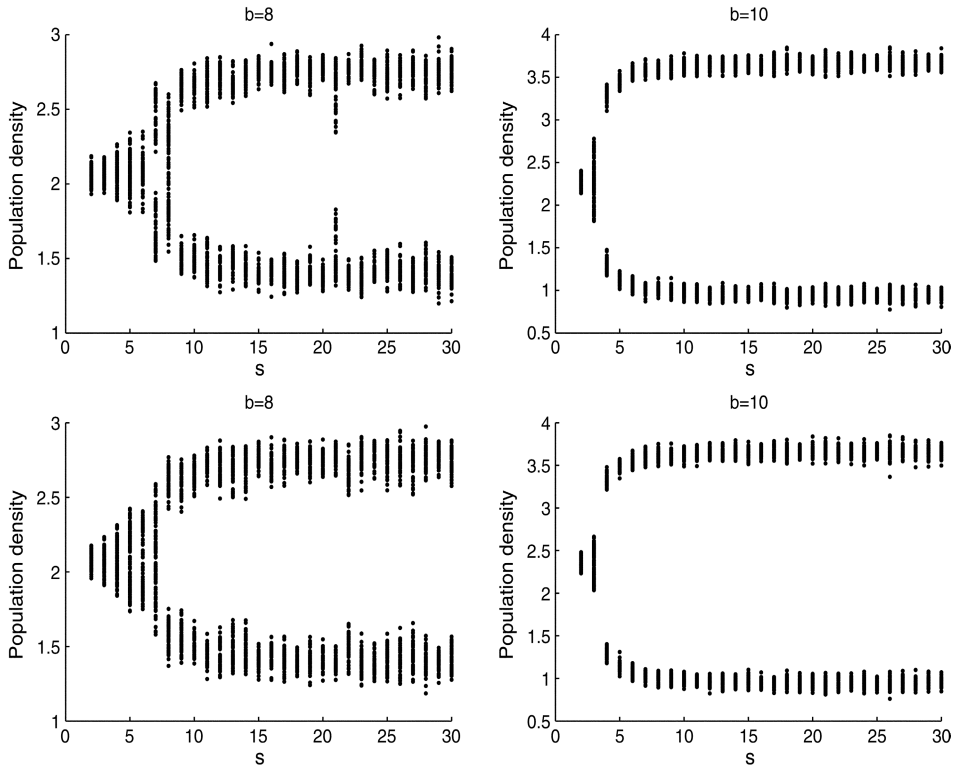

Fig. 6. 'Bifurcation plots' comparing the individual-based model (top row) and its coupled map lattice approximation (bottom row) for $b = 8$ offspring (left) and $b = 10$ offspring (right). For each s we simulated 5000 generations and plotted the population density of the last 100 generations.

$$X^{t+1} = \hat{D}(\hat{R}(X^t), \epsilon^t) \tag{13}$$

where $\hat{D} : \mathbb{R}^l \times \mathbb{R}^l \mapsto \mathbb{R}^l$ and $\hat{R} : \mathbb{R}^l \mapsto \mathbb{R}^l$ are defined below. Eq. (13) is a simplified analogue of Eq. (6), designed to have similar properties.

4.1. Reproduction

To facilitate analysis, the reproductive phase is given by a step function. Define $\hat{R} : \mathbb{R}^l \mapsto \mathbb{R}^l$ component-wise by:

$$\hat{R}_i(x) = \begin{cases} x_a & \text{if } x_i \leq x_c \\ x_b & \text{otherwise} \end{cases} \tag{14}$$

where x_i is component i of $x \in \mathbb{R}^l$. Each of the patches can have two different population levels, either high, x_a, or low, x_b, i.e., $x_a > x_b$. Assuming that $x_c \in (x_a, x_b)$ the dynamical system $x^{t+1} = \hat{R}(x^t)$ will have period 2 population dynamics, such that all patches oscillate between x_a and x_b, although not necessarily in the same phase. Such oscillations

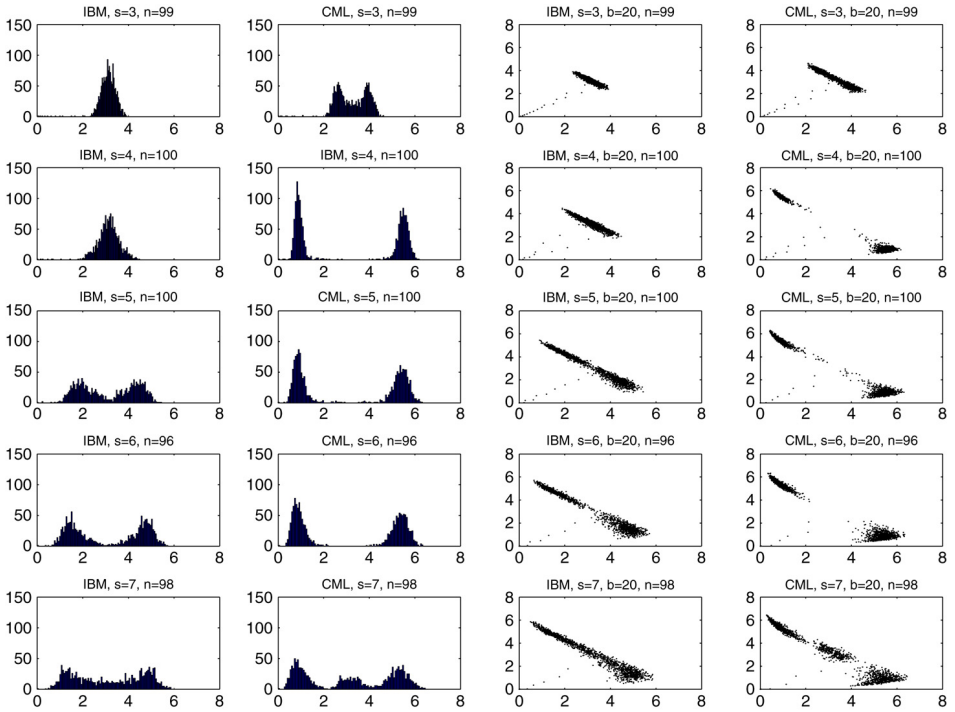

Fig. 7. Distribution plots (left) and delay plots (right) for the individual-based model (columns 1 and 3) and its coupled map lattice approximation (columns 2 and 4) for $b = 20$ and dispersal range from $s = 3$ to $s = 7$. With $b = 20$ the mean approximation, Eq. (4), has chaotic dynamics.

are typically seen for some parameter values in both the individual-based model and the coupled map lattice when $b > e^2$.

4.2. Diffusion

The patches are globally coupled, and we thus define $\hat{D}$ component-wise as

$$\hat{D}_i(x, \epsilon) = (1 - d)x_i + \frac{d}{l}\sum_{j=1}^{l} x_j + \frac{\sigma}{s^{3/2}}\epsilon_i. \tag{15}$$

The final term can be considered as representing an aggregate of stochasticity from reproduction and diffusion, giving noise that scales like the noise in the coupled map lattice approximation [see Eqs. (7) and (8)].

4.3. Population dynamics

To study the population dynamics of Eq. (13) we track the expected fraction of sites that equal x_a after the reproductive stage. Write ρ_a^t for this fraction. The expected population density given ρ_a^t is $\rho_a^t x_a + (1 - \rho_a^t)x_b$.

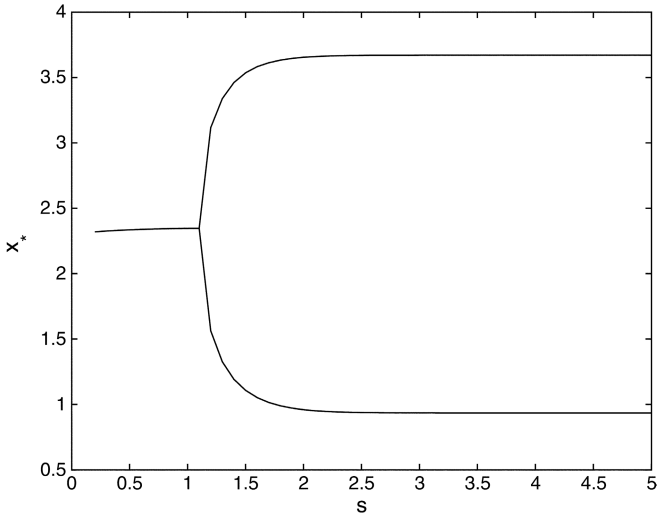

Fig. 8. 'Bifurcation plot' showing the effect of noise on periodic population dynamics in a simple and analytically tractable stochastic coupled map lattice, Eq. (13). The noise added at each site is proportional to $s^{-3/2}$ [Eq. (15)], thus scaling as in the coupled map lattice approximation. At each site the reproduction is given by Eq. (14) with $x_a = 3.6706$, $x_b = 0.9346$ and $x_c = 2.4$. These values are chosen for the dynamics to resemble Eq. (4), the Ricker map, with $b = 10$. Specifically, x_a and x_b are chosen to give the same periodic orbit, while x_c is on the boundary of the stable set to the periodic fixed points of the Ricker map with $b = 10$.

We now determine the expected value of ρ_a^{t+1} conditioned on ρ_a^t. If a site i equals x_a at time t, then stochastic diffusion changes the value to

$$(1-d)x_a + d(\rho_a^t x_a + (1-\rho_a^t)x_b) + \frac{\sigma}{s^{3/2}}\epsilon_i^t.$$

In the reproductive step the site will change to x_b if and only if

$$\epsilon_i^t > \frac{s^{3/2}}{\sigma}\left(x_c - \left((1-d)x_a + d(\rho_a^t x_a + (1-\rho_a^t)x_b)\right)\right).$$

Define

$$r_{ab}(\rho, s) = \mathrm{P}\left(\epsilon_i^t > \frac{s^{3/2}}{\sigma}\left[x_c - ((1-d)x_a + d(\rho_a^t x_a + (1-\rho_a^t)x_b))\right]\right).$$

It should be noted that r_{ab} can be interpreted as the probability that a site in state x_a will change to x_b in one iteration. As $l \to \infty$ we have

$$\rho_a^{t+1} = \rho_a^t + r_{ba}(\rho_a^t, s)(1-\rho_a^t) - r_{ab}(\rho_a^t, s)\rho_a^t. \tag{16}$$

Writing $\rho_a^{t+1} = g(\rho_a^t)$ we are interested in the fixed points for $g^2(\rho) = g(g(\rho))$, corresponding to period 2 fixed points for g.

Fig. 8 shows the expected population density for the fixed points with $d = 0.5$. When there is sufficient stochasticity there is only one fixed point, corresponding to a complete

desynchronisation of the system. As the variance decreases a bifurcation occurs and two new stable fixed points appear. As s increases, these move to x_a and x_b respectively.

This noise induced bifurcation is very possibly what causes the shift in population dynamics of the CML approximation, Eq. (6), as the dispersal range decreases. This possibility is supported by the qualitative similarity between Figs. 6 and 8. It is worth noting that Eq. (13) has global rather than local diffusion. It is thus local stochasticity, rather than spatial structure per se, that leads to the bifurcation in Figs. 6 and 8. In the individual-based model, local stochasticity and spatial structure are inseparable. The CML approximation reveals that it is the local stochasticity, in particular, that stabilises the population dynamics.

5. Discussion

Coupled map lattices are not new in ecology. They have frequently been used to model population dynamics (Hassell et al., 1991; Bascompte and Sole, 1994; Janosi and Scheuring, 1997; Keeling et al., 1997; Rees and Paynter, 1997; Yokozawa et al., 1999; Bjørnstad and Bascompte, 2001), sometimes as an alternative to spatially explicit individual-based models. The approximation proposed in this paper provides a direct link between certain spatially explicit individual-based models and stochastic coupled map lattices. Relating the two approaches is important since it effectively disentangles the deterministic and stochastic element of local interaction and dispersal, thus exposing the role of noise in producing spatial population dynamics.

In this paper we have concentrated on the specific case of scramble competition. However, a similar approach should hold for many other types of interactions. Specifically, Johansson and Sumpter (2003) considered contest competition, cooperation and predator–prey systems under uniform dispersal. These examples could easily be extended into the spatial case, and analysed through the technique presented here.

Through a series of simplifications we have reduced the spatial scramble competition model to a simple, analytically tractable counterpart, Eq. (16), which still retains the important qualitative properties (Figs. 6 and 8). This process has highlighted the importance of including a stochastic term in coupled map lattice approximations. In single species models without a stochastic term, diffusion synchronises all maps on the lattice and the approximation fails. With this stochastic term, not only is the approximation accurate, but we are also able to explain how the individual-based model behaves as we change the dispersal range. Indeed, the increased local demographic stochasticity when the dispersal range is short appears to be of particular importance in stabilising the population dynamics, over and above that of space itself.

Demographic stochasticity plays a central role in explaining why spatial structure tends to have a stabilising effect on the population dynamics. Jaggi and Joshi (2001) illustrated the stabilisation phenomena—used to explain why chaos is so infrequent in ecological time series (Hassell et al., 1976; Turchin and Taylor, 1992)—by incorporating random spatial variation into simple difference equations. They found that spatial variation could indeed have a stabilising role, but provided no convincing explanation of how spatial variation is maintained. The coupled map lattice approximation provides a simple yet

compelling explanation: stabilisation is a result of increased noise from local dispersal and competition. Furthermore, this stochasticity is self-maintaining through the generation of spatially unsynchronised patches.

The route is now clear for other spatially explicit individual-based models and stochastic coupled map lattice models to be linked through the approximation proposed here. The coupled map lattices applied thus far in ecology have, in general, been deterministic models of predator–prey interactions. Since even small perturbations can have profound effects on the dynamics of a coupled map lattice (Losson and Mackey, 1995), these deterministic models are open to the criticism that the patterns they produce, usually spiral waves, are simply an artefact of determinism. To address such criticism, Wilson et al. (1993) and Bascompte et al. (1997) have shown that individual-based models can produce the same types of spatial patterning as their deterministic counterparts. However, the form of these patterns is strongly dependent on the implementation of individual stochasticity and it is unlikely that deterministic coupled map lattices can be derived as a biologically realistic limit of the individual-based simulation (Wilson et al., 1993).

The coupled map lattice approximation can be used to solve the 'inverse problem' for deterministic coupled map lattices. Given a deterministic coupled map lattice, the interaction function for the corresponding individual-based model can be determined and the individual-based model constructed. The stochastic terms arising from the individual-based model can then be calculated. The resultant stochastic coupled map lattice can be analysed to determine whether large-scale patterns can be maintained under the assumptions necessary for a biologically realistic individual-based model. For the single species model described here it was stochasticity that produced the spatial checkerboard pattern, while for the predator–prey model described by Hassell et al. (1991) the question is whether or not stochasticity will destroy or significantly alter spiral wave patterns. Studying such systems has direct relevance to ecology, where the question as to how to translate the dynamics of populations over different scales has so far resisted a simple solution. Hopefully, the coupled map lattice approximation will strengthen our mathematical armoury as we mount further assaults on this problem.

Acknowledgements

We thank Anders Johansson for comments and ideas, Paul Glendinning for careful reviewing and correction of the manuscript, and the anonymous referee for useful suggestions. DJTS was funded by STINT, Sweden.

References

Bascompte, J., Sole, R.V., 1994. Spatially induced bifurcations in single-species population-dynamics. J. Anim. Ecol. 63, 256–264.

Bascompte, J., Sole, R.V., Martinez, N., 1997. Population cycles and spatial patterns in snowshoe hares: an individual-oriented simulation. J. Theor. Biol. 187, 213–222.

Bjørnstad, O.N., Bascompte, J., 2001. Synchrony and second-order spatial correlation in host-parasitoid systems. J. Anim. Ecol. 70, 924–933.

Boerlijst, M., Lamers, M.E., Hogeweg, P., 1993. Evolutionary consequences of spiral waves in a host-parasitoid system. Proc. R. Soc. Lond. B 253, 15–18.

Bolker, B., Grenfell, B., 1995. Space, persistence and dynamics of measles epidemics. Philos. Trans. R. Soc. Lond. B 348, 309–320.

Bolker, B., Pacala, S.W., 1997. Using moment equations to understand stochastically driven spatial pattern formation in ecological systems. Theor. Popul. Biol. 52, 179–197.

Bolker, B.M., Pacala, S.W., Levin, S.A., 2000. Moment methods for ecological processes in continuous space. In: Dieckmann, U., Law, R., Metz, J.A.J. (Eds.), The Geometry of Ecological Interactions. Cambridge University Press.

Czaran, T., 1998. Spatiotemporal Models of Population and Community Dynamics. Chapman and Hall.

DeAngelis, D.L., Gross, L.J., 1992. Individual-based Models and Approaches in Ecology: Populations Communities and Ecosystems. Chapman and Hall.

Diekmann, U., Law, R., Metz, J.A.J., 2000. The Geometry of Ecological Interactions. Cambridge University Press.

Ermentrout, G., Edelstein-Keshet, L., 1992. Cellular automata approaches to biological modelling. J. Theor. Biol. 160, 97–133.

Hassell, M.P., Comins, H.N., May, R.M., 1991. Spatial structure and chaos in insect population-dynamics. Nature 353, 255–258.

Hassell, M.P., Lawton, J.H., May, R.M., 1976. Patterns of dynamical behavior in single species populations. J. Anim. Ecol. 42, 471–486.

Iwasa, Y., Nakamaru, M., Levin, S.A., 1998. Allelopathy of bacteria in a lattice population: Competition between colicin-sensitive and colicin-producing strains. Evol. Ecol. 12, 785–802.

Jaggi, S., Joshi, A., 2001. Incorporating spatial variation in density enhances the stability of simple population dynamics models. J. Theor. Biol. 209, 249–255.

Janosi, I.M., Scheuring, I., 1997. On the evolution of density dependent dispersal in a spatially structured population model. J. Theor. Biol. 187, 397–408.

Johansson, A., Sumpter, D.J.T., 2003. From local interactions to population dynamics in site-based models of ecology. Theor. Popul. Biol. 64, 497–517.

Johnson, C.R., Boerlijst, M.C., 2002. Selection at the level of the community: the importance of spatial structure. Trends Ecol. Evol. 17, 83–90.

Keeling, M.J., Mezic, I., Hendry, R.J., McGlade, J., Rand, D.A., 1997. Characteristic length scales of spatial models in ecology via fluctuation analysis. Philos. Trans. R. Soc. Lond. B 352, 1589–1601.

Keeling, M.J., Wilson, H.B., Pacala, S.W., 2000. Reinterpreting space, time lags, and functional responses in ecological models. Science 290, 1758–1761.

Keeling, M.J. et al., 2001. Dynamics of the 2001 UK foot and mouth epidemic: Stochastic dispersal in a heterogeneous landscape. Science 294, 813–817.

Kerr, B., Riley, M.A., Feldman, M.W., Bohannan, B.J.M., 2002. Local dispersal promotes biodiversity in a real-life game of rock-paper-scissors. Nature 418, 171–174.

Losson, J., Mackey, M.C., 1995. Evolution of probability densities in stochastic coupled map lattices. Phys. Rev. E (3) 52, 1403–1417.

May, R.M., 1976. Simple mathematical models with very complicated dynamics. Nature 261, 459–467.

Mollison, D., 1991. Dependence of epidemic and population velocities on basic parameters. Math. Biosci. 107, 255–287.

Murray, J.D., 1989. Mathematical biology. In: Biomathematics, vol. 19, Springer, Berlin.

Nicholson, A.J., 1954. An outline of the dynamics of animal populations. Austr. J. Zool. 2, 9–65.

Nowak, M.A., May, R.M., 1992. Evolutionary games and spatial chaos. Nature 359, 826–829.

Pacala, S.W., Tilman, D., 1996. Limiting similarity in mechanistic and spatial models of plant competition in heterogeneous environments. Am. Nat. 143, 222–257.

Pascual, M., Levin, S.A., 1999. From individuals to population densities: Searching for the intermediate scale of nontrivial determinism. Ecology 80, 2225–2236.

Rand, D.A., Wilson, H.B., 1995. Using spatio-temporal chaos and intermediate-scale determinism to quantify spatially extended ecosystems. Proc. R. Soc. Lond. B 259, 111–117.

Rees, M., Paynter, Q., 1997. Biological control of scotch broom: modelling the determinants of abundance and the potential impact of introduced insect herbivores. J. Appl. Ecol. 34, 1203–1221.

Ricker, W.E., 1954. Stock and recruitment. J. Fisher. Res. Board Can. 11, 559–623.

Sato, K., Iwasa, Y., 2000. Pair approximations for lattice-based ecological models. In: Dieckmann, U., Law, R., Metz, J.A.J. (Eds.), The Geometry of Ecological Interactions. Cambridge University Press.

Sumpter, D.J.T., Broomhead, D.S., 2001. Relating individual behaviour to population dynamics. Proc. R. Soc. Lond. B 268, 925–932.

Thunberg, H., 2001. Periodicity versus chaos in one-dimensional dynamics. SIAM Rev. 43, 3–30.

Toquenaga, Y., Fujii, K., 1991. Contest and scramble competition between two bruchid species (coleoptra: Bruchidae) 2. Larval competition experiment. Resour. Popul. Ecol. 33, 129–139.

Turchin, P., Taylor, A.D., 1992. Complex dynamics in ecological time series. Ecology 73, 289–305.

van Baalen, M., 2000. Pair approximations for different spatial geometries. In: Dieckmann, U., Law, R., Metz, J.A.J. (Eds.), The Geometry of Ecological Interactions. Cambridge University Press.

Wilson, W.G., Deroos, A.M., Mccauley, E., 1993. Spatial instabilities within the diffusive lotka-volterra system—individual-based simulation results. Theor. Popul. Biol. 43, 91–127.

Yokozawa, M., Kubota, Y., Hara, T., 1999. Effects of competition mode on the spatial pattern dynamics of wave regeneration in subalpine tree stands. Ecol. Model. 118, 73–86.